A mini review on factors affecting particle size, sphericity and pore size of mesoporous silica nanoparticles

Jemal Dilebo

Department of Pharmaceutics and Social Pharmacy,
School of Pharmacy, College of Health Sciences, Addis Ababa University, Ethiopia
Email: jdilebo@gmail.com
Mobile phone: 251913021659

Abstract - There are two main classes of mesoporous silica nanoparticles (MSN) and these are M41S and SBA. They have diverse fields of applications such as drug delivery, catalysis, separation and sorption. In their synthesis the major types of reagents used are silica precursor, structure directing agent/surfactant, catalyst and water. This mini review elaborates on the conditions which could affect particle size, sphericity, pore size and pore wall thickness of MSN in relation to molar ratios of the reagents, synthesizing conditions, use of cosurfactants and cosolvents.

Key words: mesoporous silica nanoparticles, particle size, sphericity, pore size

Introduction

There are different types of mesoporous silica naoparticles (MSN) which mainly differ in the geometry of their mesostructures. The first types of these novel materials have been given the name M41S and include MCM-41, MCM-48, and MCM-50. MCM-41 (Mobil Crystalline Material-41) is the first type of M41S synthesized by Mobil Corporation in 1992. The M41S family of mesopoures materials can be synthesized by using various experimental conditions [1]. MSN have applications in different fields such as drug delivery, catalysis, separation and sorption [2].

The basic synthetic reagents of MSN are silica precursors (e.g., tetraethyl orthosilicate (TEOS), tetramethyl orthosilicate (TMOS), tetrabutyl orthosilicate (TBOS), and sodium silicate), structure directing agents (e.g., hexadecyltrimethylammonium bromide/chloride/hydroxide (CTAB/Cl/OH), Pluronic P123 and Pluronic F127); catalysts (e.g., sodium hydroxide, hydrochloric acid, ammonia, and triethanoleamine) and water. Water is also important as highly diluted aqueous media favors assembly of MSN [3]. At less amount of water, no siliceous material was formed [4].

In order to modify the morphology and particle size of the synthesized MSN, cosurfactants and cosolvents are also used. For example, Pluronic F127 inhibited particle size growth of MCM-41 and MCM-48 when used as a cosurfactant along with a cationic surfactant [5-6]. The use of increasing concentration of ethanol resulted in progressive synthesis of MCM-41, MCM-48, MCM-50 and a radial hexagonally ordered phase. The formed spheres displayed cubic pores in the central region and hexagonal geometry at the periphery [7-8].

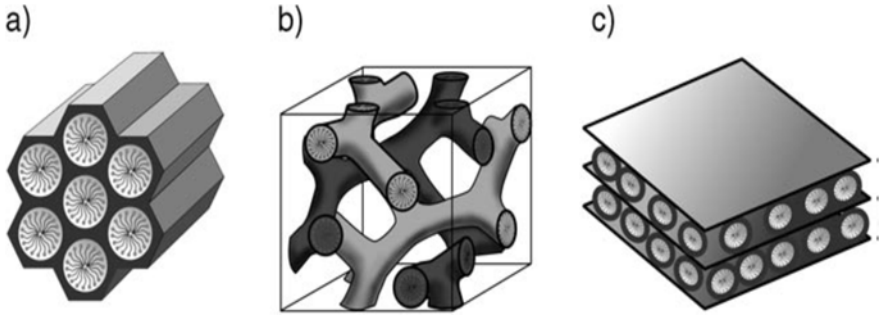

Figure 1. Structures of mesoporous M41S materials: a) MCM-41 (hexagonal); b) MCM-48 (cubic); c) MCM-50 (lamellar) [9].

MCM-41

MCM-41 (figure 1a) has 2D hexagonal mesopore structure and prepared under basic conditions at pH 8.5-12 using cationic surfactants [10]. Under X-ray diffraction MCM-41 produces 3-5 peaks which indexes hexagonal lattice [11]. The pore walls of MCM-41 are formed from amorphous silica as characterized by XRD measurements [12]. MCM-41 displays the typical (100) and (110) peaks due to an ordered hexagonal (P6 mm) network of mesopores along with weak (200) and (201) peaks showing the long range order of the structure. Upon functionalization of MCM-41 with NH_2 the intensity of the latter peaks decreases [13].

At cationic surfactant to silica ratio of less than 1, the major synthesized mesoporous material appeared to be hexagonal phase MCM-41. As the ratio of the surfactant to silica increased above 1, a cubic phase (i.e., MCM-48) can be formed. As the concentration ratio of surfactant to silica ratio increases further, another material called MCM-50 forms [11]. A high stirring rate of about 850 rpm can cause mesostructure change from MCM-41 to MCM-48 [6].

MCM-41 with different types of morphologies such as rods, gyroids, discoids, nano-fibers, helix, and spheres have been successfully synthesized [14-18]. Morphologies of MCM-41 such as rods, spirals or closed loops are formed at acidic conditions [19].

The MCM-41 aging time during synthesis was reduced to 2 hrs [20] despite longer time up to 48 hrs needed in the previous studies. Shi et al [21] were able to prepare MCM-41 with size of 10-60 nm using highly diluted solutions of TEOS and CTAB 12.45mM and 1.52mM, respectively.

MCM-48

MCM-48 (figure 1b) has a 3D cubic mesostructure and prepared under basic conditions using cationic surfactants. Unlike MCM-41, MCM-48 has interwoven and branched pore structure, which is more suitable for mass transfer kinetics than MCM-41 which has unidirectional pore system [22].

SBA-15 and SBA-16

SBA-15 has a 2D hexagonal mesostructure and prepared under acidic conditions using triblock copolymer Pluronic (poly (ethylene oxide) poly(propylene oxide) poly(ethylene oxide)). SBA type of mesoporous materials have pore diameter in the range 2-30 nm, which is larger than M41S type of mesoporous materials. SBA-15 has also pores which connect parallel mesopores and micropores which emanate from the mesopores. The size of the micropores could range from 1nm up to 5 nm [23]. The formation of connecting pores in SBA-15 is attributed to the silicate penetrating characteristics of poly(ethylene oxide) block of the Pluronic. Such pores can be closed when calcinating SBA- 15 at a temperature above 1173 K [24].

SBA-16 is SBA-15 like mesostructure but with 3D mesopores with approximate pore size 5-15 nm and corresponding to the space group Im3m and synthesized under acidic conditions using Pluronic as structure directing agent [25].

Mechanisms of formation of MSNs

When a silica precursor is added to aqueous solution of cationic surfactant, white precipitate of silica-surfactant complex called MCM-41 precursor which later becomes MCM-41 upon calcination is formed [26]. Naono et al [26] stated that the primary silica oligomer that binds with the cationic surfactant to be $(HSiO_3)_n^{n-}$. Upon the adsorption of the silicate anion on the rod-like micelles of cationic surfactant, electrical neutrality prevails. Then these rod-like micelles with electrical neutrality are rapidly aggregated by the effect of van der Waals attractive force. Naono et al [26] postulated that the white precipitate mentioned above is the rapidly aggregated, electrically neutral, rod-like micelles covered with the silicate polymer $(HSiO_3)_n^{n-}$. Upon the aggregation of rod-like micelles, a hexagonally packed arrangement is most likely to form from the viewpoint of stability, because the van der Waals attractive force between the rod-like micelles is highest in the hexagonal array.

Naono et al [26] also described the following reaction mechanisms for the formation of $(HSiO_3)_n^n$ from SiO_2 (silica particle) and $Si(OR)_4$ silica precursors, respectively.

$$nSiO_2 \text{ (silica particles)} + nOH^- = (HSiO_3)_n^{n-} \text{ ……..…….(1)}$$

$$nSi(OR)_4 + nOH^- + 2nH_2O = (HSiO_3)_n^{n-} + 4nROH\text{….. (2)}$$

There are three proposed mechanisms for the formation of mesoporous nanomaterials and these include liquid crystal template, self-assembly and cooperative self-assembly mechanisms.

Liquid crystal template mechanism: Surfactant liquid crystal structures serves as template for inorganic silica. The surfactant molecules cluster to form hexagonal cylinder in which the polar groups of the surfactant projects toward the continuous water phase and the alkyl chain aggregates into the inside. Because of the electrostatic effect, the oppositely charged silicate deposits on the surface of the hexagonal cylinders and forms the wall [27]. Alternatively, it could be the silica precursor which initiate formation of liquid crystal phase/template. In either conditions, the resultant silicate encapsulated hexagonal structure produces MCM-41 [11]. After the formation of ordered arrays, thermal process is used to remove the template and produce stable mesoporous material [27].

However, there are studies highlighting preexisting liquid crystalline templates are not required for the formation of mesopourus particles [28].

Self-assembly mechanism: When the cationic surfactant and silica precursor are mixed at the initial phase at particular pH, the silica precursor converts to anionic species. Then ion exchange takes place between Br^- or OH^- and anionic silica oligomer. This ionic exchange will leads to the formation of inorganic-organic self-assembled silicate micelles (SSMs). SSMs might not form at surfactant conditions used in the absence of silicate oligomers. Finally the deposition of the SSMs leads to MCM-41[29].

Cooperative self-assembly mechanism: Cooperative interactions between inorganic and organic species can result in range of structures that would not be found in surfactant or inorganic systems alone [30]. The fact that the MSN can be formed in a mixture containing 0.5% concentration of surfactant shows that at low concentrations a cooperative templating process takes place [31].

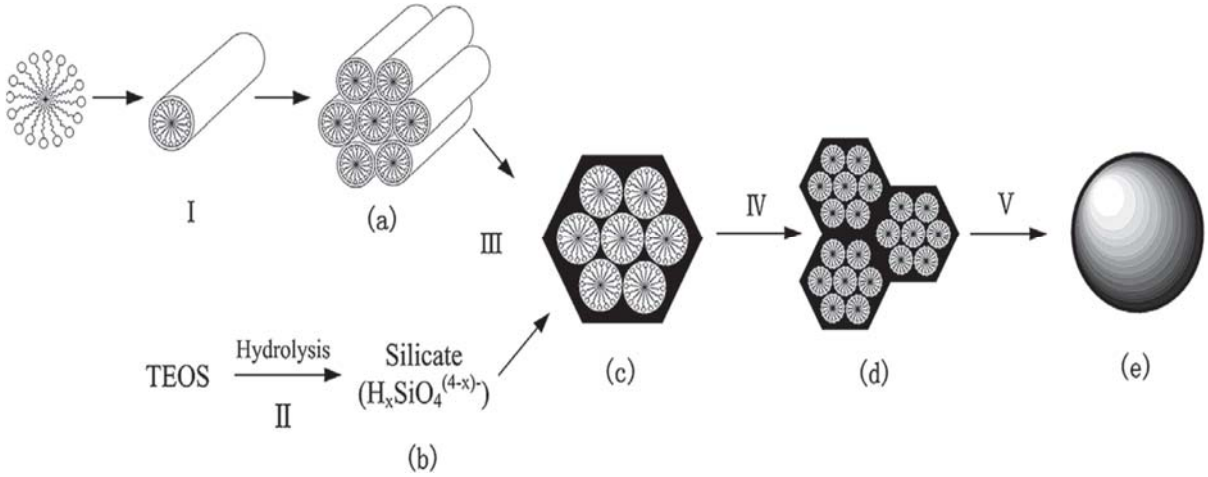

Figure 2. The formation mechanism of the mesoporous silica nanospheres [32].

Methods of removal of templates

After the synthesis of MSN the organic template can be removed by calcination or facile extraction. Calcination process burns of the surfactant template leading formation of hollow cylinders of inorganic material [27]. However, when the partice size of MSN 20-100 nm is calcined, aggregation of particles results which is difficult to redisperse as isolated nanoparticles in colloidal solution. In order to solve this problem using solvent extraction, hydrogen peroxide oxidation, or dialysis can be applied [33-35]. But the nanoparticles treated in this manner lack silica network condensation. Moreover such MSN particles have low stability in aqueous media and cause problem in application such as drug delivery [36].

It is also possible to remove template structure to some extent from mesoporous materials using water or ethanol. However, these solvents were observed to cause structural shrinkage of SBA-15 material when used to remove Pluronic 123 template. This is attributed to the removal/reduction of EO block from the silica walls upon washing and later causes void spaces, thus causing structural shrinkage [37]. In a work by Lu et al [38] template was removed using solution of hydrochloric acid and ethanol at 60 ^{o}C for 6 hrs three times and followed by drying in vacuum for overnight.

Factors affecting particle size of MSN

During synthesis of MCM-41 using CTACl and NH_4OH, Ikari et al [39] found that particle size increased with an increasing concentration of NH_4OH and decreased with decreasing concentration of NH_4OH and increased concentration of CTACl. The reason for this was explained. The decrease in the concentration of NH_4OH, reduces the pH and thus the rate of hydrolysis of TEOS and thereby the concentration of silicate anion and then resulted in the presence of excess positively charged CTA^+. The excess CTA^+ covers the composite particles and reduces particle size in similar manner to CTA^+Cl^-. The reduced particle size at increasing concentration of CTACl was thought to be due to the deposition of CTACl as neural species (CTA^+Cl^-) on CTA-silicate composite and restricts particle growth [39].

On another study by Beltrán-Osuna et al [40], MSNs size tend to increase with increase in NaOH concentration and it was stated that NaOH concentration was the major variable affecting MSNs particle size. Chen et al [32] also observed that an increase in the molar ratio of NaOH to TEOS caused an increase in the particle size of mesospheres. Wanyika et al [4] stated that the concentration ratio of NaOH with respect to other reagents should be kept in certain ratio to get good quality MSN. The authors also elaborated that the high concentration of the catalyst facilitates higher rate of precursor hydrolysis which leads to higher rate of particle size growth than nucleation rate.

Yamada et al [41] also found that the particle size of MSN decreased upon increasing cationic surfactant to silica ratio. This was explained as the nucleation rate of mesostructured material dominates particle growth rate. Rapid nucleation rate favors formation of smaller particles [19].

Lv et al [42] observed that when stirring rate was increased from 100 rpm to700 rpm, particle size was decreased from 110 nm to 38 nm. They also observed that when the stirring rate was further increased from 700 rpm to 1000 rpm, the MSN size did not decrease further. The explanation about the effect of stirring speed on the particle size was made. At low stirring rate the concentration of hydrolyzed silica at the surface of TEOS (oil phase) is greater than in the inner solution of TEOS and hence accumulation of TEOS and leads to large particle size of MSN. At high stirring rate, the concentration of silica hydrolyzed is lower at the surface and hence MSN with small particle size is formed. In addition to this stirring facilitates formation of increased quantity of nuclei which logically would lead to formation of small particles.

Smaller and relatively spherical particles were obtained in higher reaction volumes than lower reaction volumes and MSN formed in open systems tended to be larger [40].

Particle size of MSN was increased from 21 nm to 38 nm when the reaction temperature was increased from 40 ^{o}C to 95 ^{o}C. The reason for an increase in particle size with an increase in temperature is that at higher temperature the rate of hydrolysis of TEOS increases and this leads to growth of particles [40].

Stevens et al [43] was able to synthesize thick-walled, highly porous SBA-16 macro and microspheres, using nonionic surfactant and low concentration HCl (i.e., 0.4 M) in the presence of butanol as a cosolvent. The size of the microspheres synthesized was modulated by altering the amount of butanol.

Factors affecting sphericity of MSN

Spherical MCM-41 favorably forms in basic conditions which could be due to the dependence of TEOS hydrolysis and condensation on the basicity of the surrounding environment [44]. Close to spherical particles and monodispersed particle size distribution was obtained when stirring rate was 500 rpm, reaction volume 500 mL in a partially opened system for 2 hrs at 80 ^{o}C [40]. Similarly in MCM-41 synthesis, sphericity was improved when CTAB concentration was lower [45]. At 0.1% concentration of CTAB, sphericity of the MCM-41 was improved and the mesostructures also had smaller particle size and narrow size distribution [45]. Chen et al [32] was able to synthesize nanospheres of MCM-41 with fixed diameter by modulating molar ratio of NaOH/TEOS and other synthetic conditions.

Spherical SBA-15 and SBA-16 can be synthesized using mixtures of non ionic and ionic surfactants under strong acidic conditions [46-48]. Spherical SBA-15 particles were also prepared with CTAB as a cosurfactant and ethanol as a cosolvent [49]. Alcohol has an effect on sphericity of particles and ordering of pore [50-51]. When ammonia is used as a catalyst would favor spherical morphology [52].

Spherical MCM-41 particles could also be synthesized by a pseudomorphic synthesis route, in which pre-formed silica spheres are transformed into MCM-41 with the identical spherical morphology by hydrothermal treatment in surfactant solution under alkaline conditions [53].

Relatively spherical and smaller particles were also obtained at higher stirring rates than lower stirring rates [32, 40]. However, the distribution of the sphere diameters becomes more regular as the stirring rate increased from 200 rpm to 300 rpm but it became less regular when stirring rate was further increased [32]. The deterioration of the regularity under higher stirring rate could be due to destructive shearing force originated from mechanical stirring. Therefore, an appropriate stirring rate is necessary in the preparation of MCM-41 nanospheres with regular distribution [32].

Factors affecting pore size and pore wall thickness

MSNs pore size and pore volume tend to increase with an increase in carbon chain length of surfactant which serves as a template [32]. Pore size can be increased also by the use of expander compounds such as 1, 3, 5-trimethylbenzene or linear hydrocarbons [54]. 1,3,5-trimethylbenzene solvate in silicate-template aggregates because of their sheer size and increase the width of template rod and thus the pore diameter [11, 55].

Pore size was also found to increase when the as-synthesized particles were incubated in ulatrapure water at increased temperature from 25 to 70 ^{o}C and water thought to partially dissolve the less condensed inner section than the outer layer [56].

On the other hand, co-surfactants such as alcohol decrease pore size of amine-templated silica [19].

Pore wall thickness increases with decreasing concentration of the surfactant. This phenomenon was explained by the authors based on Si to CTAB molar ratio. At low concentration of CTAB, the rods formed by several layers of silica are synthesized and aggregate into organic-inorganic cylinders forming a 2D structure. Whereas at high concentration, the corresponding amount of silica precursor per CTAB decreases significantly and condenses around the cylindrical micelles formed by CTAB molecules and results in decrease in pore wall thickness [45].

Conclusion

The literature review has shown that an increase in molar ratio of catalyst to silica precursor, an increase in molar ratio of catalyst to surfactant, an increase in incubation temperature tend to increase particle size of MSN; whereas an increase in molar ratio of surfactant to silica precursor, higher stirring rate and large volume of reaction tend to decrease MSN particle size. Pore sizes or volumes of MSN was expanded by the use of 1,3,5 trimethylbenzene and surfactants with longer carbon chain. Use of cosolvents such as ethanol and cosurfactants have been employed to synthesize spherical MSN.

References

[1] F. Di Renzo, H. Cambon, and R. Dutartre. A 28-year-old synthesis of micelle-templated mesoporous silica. Microporous Materials, 1997, 10: 283-286.

[2] H.I. Melendez-Ortizn, L.A. García-Cerda, Y. Olivares-Maldonado, et al. Preparation of spherical MCM-41 molecular sieve at room temperature: Influence of the synthesis conditions in the structural properties. Ceram. Int., 2012, 38: 6353–6358.

[3] C. Feldmann and H. Goesmann. Nanoparticulate Functional Materials. Angew. Chem. Int. Ed., 2010, 49: 1362 -1395.

[4] H. Wanyika, E. Gatebe, P. Kioni, et al. Synthesis and characterization of ordered mesoporous silica nanoparticles with tunable physical properties by varying molar composition of reagents. African Journal of Pharmacy and Pharmacology, 2011, 5: 2402-2410.

[5] K. Ikari, K.Suzuki, and H. Imai. Structural Control of Mesoporous Silica Nanoparticles in a Binary Surfactant System. Langmuir, 2006, 22: 802-806.

[6] T.W. Kim, P. W. Chung, and V.S.Y. Lin. Facile Synthesis of Monodisperse Spherical MCM-48 Mesoporous Silica Nanoparticles with Controlled Particle Size. Chem. Mater., 2010, 22: 5093–5104.

[7] G. Van Tendeloo, O. I. Lebedev, O. Collart, et al. Structure of nanoscale mesoporous silica spheres. J. Phys. Cond. Matter, 2003, 15: S3037.

[8] O. I. Lebedev, G.Van Tendeloo, O. Collart, et al. Structure and microstructure of nanoscale mesoporous silica spheres. Solid State Sci., 2004, 6: 489-498.

[9] F. Hoffmann, M. Cornelius, J. Morell, et al. Silica-Based Mesoporous Organic–Inorganic Hybrid Materials. Angew. Chem. Int. Ed., 2006, 45: 3216 – 3251.

[10] A.C. Voegtlin, A. Matijasic, J. Patarin, et al. Room-temperature synthesis of silicate mesoporous MCM-41 –type materials: influence of the synthesis pH on the porosity of the materials obtained. Microporous Materials, 1997, 10:137-147.

[11] J. S. Beck, J. C. Vartuli, W. J. Roth, et al. A New Family of Mesoporous Molecular Sieves Prepared with Liquid Crystal Templates. J. Am, Chem. Soc., 1992, 114: 10834-10843.

[12] M. Grün, I. Lauer, and K. K.Unger. The Synthesis of Micrometer- and Submicrometer-Size Spheres of Ordered Mesoporous Oxide MCM-41. Adv. Mater., 1997, 9: 254-257.

[13] P. Iliade, I. Miletto, S. Coluccia, et al. Functionalization of mesoporous MCM-41 with aminopropyl groups by co-condensation and grafting: a physico-chemical characterization. Res Chem Intermed, 2012, 38:785–794.

[14] Q.S. Huo, D.I. Margolese, U. Ciesla, et al. Organization of Organic Molecules with Inorganic Molecular Species into Nanocomposite Biphase Arrays. Chem. Mater., 1994, 6 :1176-1191.

[15] F. Marlow, M. D. McGehee, D. Y. Zhao, et al. Doped Mesoporous Silica Fibers: A New Laser Material. Adv. Mater., 1999, 11: 632-636.

[16] A. Galarneau, J. Iapichella, K. Bonhomme, et al. Controlling the Morphology of Mesostructured Silicas by Pseudomorphic Transformation: a Route Towards Applications. Adv. Funct. Mater., 2006,16: 1657-1667.

[17] S. Yang, L. Zhao, C. Yu, et al. On the Origin of Helical Mesostructures. J. Am. Chem. Soc., 2006, 128: 10460-10466.

[18] K. Ishikawa, T. Akasaka, Y. Yawaka, et al. High Functional Expression of Osteoblasts on Imogolite, Aluminosilicate Nanotubes. J. Biomed. Nanotechnol., 2010, 6: 59-65.

[19] F. Di Renzo, F. Testa, J.D. Chen, et al. Textural control of micelle-templated mesoporous silicates: the effects of co-surfactants and alkalinity. Microporous Mesoporous Mater., 1999, 28:437–446.

[20] X. Liu, H. Sun, and Y. Yang. Rapid synthesis of highly ordered Si-MCM-41. . J. Colloid Interface Sci, 2008, 319: 377–380.

[21] Y.T Shi, H. Y. Cheng, Y. Geng, et al. The size-controllable synthesis of nanometer-sized mesoporous silica in extremely dilute surfactant solution. Mater. Chem. Phys., 2010, 120: 193–198.

[22] K. Schumacher, M. Grün, and K.K. Unger. Novel synthesis of spherical MCM-48. Microporous Mesoporous Mater., 1999, 27: 201–206.

[23] A. Galarneau, H. Cambon, F. Di Renzo, et al. Microporosity and connections between pores in SBA-15 mesostructured silicas as a function of the temperature of synthesis. New J. Chem., 2003, 27: 73–79.

[24] J.R. Matos, L.P. Mercuri, M.Kruk, et al . Toward the Synthesis of Extra-Large-Pore MCM-41 Analogues. Chem. Mater., 2001, 13: 1726-1731.

[25] G. F. Andrade, D. C. F. Soares, R. G. dos Santos, et al. Mesoporous silica SBA-16 nanoparticles: Synthesis, physicochemical characterization, release profile, and in vitro cytocompatibility studies. Microporous Mesoporous Mater., 2013,168:102–110.

[26] H. Naono, M. Hakuman, T. Tsunehisa, et al. Formation Process of MCM-41 Precursor and Porous Texture of MCM-41. J. Colloid Interface Sci., 2000, 224: 358–365.

[27] C.T. Kresge, M.E. Leonowicz, W.J.Roth, et al. Ordered mesoporous molecular sieves synthesized by a liquid-crystal template mechanism. Nature, 1992, 359: 710-712.

[28] R. Zana, J. Frasch, M. Soulard, et al. Fluorescence Probing Investigations of the Mechanism of Formation of Organized Mesoporous Silica. Langmuir, 1999, 15: 2603-2606.

[29] Q. Cai, Z. S. Luo, W. Q. Pang, et al. Dilute Solution Routes to Various Controllable Morphologies of MCM-41 Silica with a Basic Medium. Chem. Mater., 2001, 13: 258-263.

[30] A. Firouzi, D. Kumar, L. M. Bull, et al. Cooperative Organization of Inorganic-Surfactant and Biomimetic Assemblies. Science, 1995, 267:1138-1143.

[31] K.W. Gallis and C. C. Landry. Synthesis of MCM-48 by a Phase Transformation Process. Chem. Mater., 1997, 9: 2035-2038.

[32] Y. Chen, X. Shi, B. Han, et al.. The Complete Control for the Nanosize of Spherical MCM-41. J. Nanosci. Nanotechnol., 2012, 12: 7239–7249.

[33] V. Cauda, A. Schlossbauer, J. Kecht, et al. Multiple core-shell functionalized colloidal mesoporous silica nanoparticles. J. Am. Chem. Soc., 2009, 131: 11361–11370.

[34] C. Urata, Y. Aoyama, A. Tonegawa, et al. Dialysis process for the removal of surfactants to form colloidal mesoporous silica nanoparticles. Chem. Commun., 2009, 34: 5094–5096.

[35] J. Kecht and T. Bein. Oxidative removal of template molecules and organic functionalities in mesoporous silica nanoparticles by H_2O_2 treatment. Microporous Mesoporous Mater., 2008, 116: 123–130.
[36] V. Cauda, C. Argyo, D. G. Piercey, et al. "Liquid-Phase Calcination" of Colloidal Mesoporous Silica Nanoparticles in High-Boiling Solvents J. Am. Chem. Soc., 2011, 133: 6484–6486.
[37] M. Kruk, M. Jaroniec, C. H. Ko, et al. Characterization of the Porous Structure of SBA-15. Chem. Mater., 2000, 12: 1961-1968.
[38] Y. Lu, Y. Yang, Z. Gu, et al. Glutathione-depletion mesoporous organosilica nanoparticles as a self-adjuvant and Co-delivery platform for enhanced cancer immunotherapy. Biomaterials, 2018, 175:82-92.
[39] K. Ikari, K. Suzuki, and H. Imai. Grain Size Control of Mesoporous Silica and Formation of Bimodal Pore Structures. Langmuir, 2004, 20: 11504-11508.
[40] Á.A. Beltrán-Osuna, J. L. G. Ribelles, and J. E. Perilla. A study of some fundamental physicochemical variables on the morphology of mesoporous silica nanoparticles MCM-41 type. J Nanopart Res., 2017, 19 : 381.
[41] H.Yamada, C. Urata, S. Higashitamori, et al. Critical Roles of Cationic Surfactants in the Preparation of Colloidal Mesostructured Silica Nanoparticles: Control of Mesostructure, Particle Size, and Dispersion. ACS Appl. Mater. Interfaces, 2014, 6: 3491−3500.
[42] X. Lv, L. Zhang, F Xing, et al. Controlled synthesis of monodispersed mesoporous silica nanoparticles: Particle size tuning and formation mechanism investigation. Microporous Mesoporous Mater., 2016, 225: 238-244.
[43] W.J. J. Stevens, K. Lebeau, M. Mertens, et al. Investigation of the Morphology of the Mesoporous SBA-16 and SBA-15 Materials. J. Phys. Chem. B, 2006, 110: 9183-9187.
[44] T. Nakamura, M. Mizutani, H. Nozaki, et al. Formation Mechanism for Monodispersed Mesoporous Silica Spheres and Its Application to the Synthesis of Core/Shell Particles. J. Phys. Chem. C, 111: 1093-1100.
[45] G. Lelong, S. Bhattacharyya, S. Kline, et al. Effect of Surfactant Concentration on the Morphology and Texture of MCM-41 Materials. J. Phys. Chem. C, 2008, 112: 10674–10680.
[46] D. Zhao, J. Sun, Q. Li, et al. Morphological Control of Highly Ordered Mesoporous Silica SBA-15. Chem. Mater., 2000, 12: 275-279.
[47] B. C. Chen, M. C. Chao, H. P. Lin, et al. Faceted single crystals of mesoporous silica SBA-16 from a ternary surfactant system: surface roughening model. Microporous Mesoporous Mater., 2005, 81: 241-249.
[48] M. Mesa, L. Sierra, B. López, et al. Preparation of micron-sized spherical particles of mesoporous silica from a triblock copolymer surfactant, usable as a stationary phase for liquid chromatography. Solid State Sci., 2003, 5: 1303-1308.
[49] A. Katiyar, S. Yadav, P. G. Smirniotis, et al. Synthesis of ordered large pore SBA-15 spherical particles for adsorption of biomolecules. J.Chromatogr. A, 2006, 1122: 13–20.
[50] S. Liu, P. Cool, O. Collart, et al. The Influence of the Alcohol Concentration on the Structural Ordering of Mesoporous Silica: Cosurfactant versus Cosolvent. J. Phys. Chem. B, 2003, 107: 10405-10411.
[51] S. Liu, L. Lu, Z. Yang, et al. Further investigations on the modified Stöber method for spherical MCM-41. Mater. Chem. Phys., 2006, 97: 203-206.
[52] W. Stober, A. Fink, and E. Bohn. Controlled Growth of Monodisperse Silica Spheres in the Micron size range. J. Colloid Interface Sci., 1968, 26: 62-69.
[53] T. Martin, A. Galarneau, F. Di Renzo, et al. Morphological Control of MCM-41 by Pseudomorphic Synthesis. Angew. Chem. Int. Ed., 2002, 14: 2590-2592.
[54] N. Ulagappan, and C. N. R. Rao. Evidence for supramolecular organization of alkane and surfactant molecules in the process of forming mesoporous silica. Chem. Commun., 1996, 2759-2760.
[55] Q. S. Huo, D. Y. Zhao, J. Feng, et al. Room temperature growth of mesoporous silica fibers: A new high surface area optical waveguide. Adv. Mater., 1997, 9:974-978.
[56] X. Wang, X. Li, A. Ito, et al. Hollow Structure Improved Anti-Cancer Immunity of Mesoporous Silica Nanospheres In Vivo. Small, 2016, 12: 3510-3515.